

Quantum Monte Carlo Study of an Interaction-Driven Band-Insulator-to-Metal Transition

N. Paris,¹ K. Bouadim,² F. Hebert,² G. G. Batrouni,² and R. T. Scalettar¹

¹Physics Department, University of California, Davis, California 95616, USA

²Institut Non-Linéaire de Nice, UMR 6618 CNRS, Université de Nice-Sophia Antipolis,
1361 route des Lucioles, 06560 Valbonne, France

(Received 26 July 2006; published 25 January 2007)

We study the transitions from band insulator to metal to Mott insulator in the ionic Hubbard model on a two-dimensional square lattice using determinant quantum Monte Carlo. Evaluation of the temperature dependence of the conductivity demonstrates that the metallic region extends for a finite range of interaction values. The Mott phase at strong coupling is accompanied by antiferromagnetic order. Inclusion of these intersite correlations changes the phase diagram qualitatively compared to dynamical mean field theory.

DOI: 10.1103/PhysRevLett.98.046403

PACS numbers: 71.10.Fd, 02.70.Uu, 71.30.+h

Introduction.—Interaction effects in tight-binding models such as the Hubbard Hamiltonian have been widely studied, and understood, for their ability to drive transitions to magnetically ordered states and insulating behavior. There has been considerable interest, but no clear consensus, concerning the possibility of a converse phenomenon, namely, that correlations can cause metallic behavior. The insulating starting point in most such studies has been a phase in which the electrons are localized by disorder [1]. However, a simpler context in which to study interaction-driven insulator-to-metal transitions is to begin with a band insulating (BI) state, in which the insulating behavior is caused by a periodic external potential as opposed to a random one [2,3]. Such transitions have been conjectured to explain the enhanced response of quasi-one-dimensional correlated electron systems such as ferroelectric perovskites [4] and organic materials [5], and studied theoretically there [6], as well as nonlinear electronic polarizability in transition metal oxides [7].

Recently, this issue has been addressed in higher dimension within dynamical mean field theory (DMFT) and a number of interesting conclusions emerged [8]. However, because DMFT treats only a single site (retaining, however, all the dynamical fluctuations of the self-energy which is ignored in conventional, static mean field theory), it is important to undertake complementary work which is able to retain intersite fluctuations.

In this Letter, we investigate such BI-metal transitions with determinant quantum Monte Carlo (DQMC). We study the “ionic Hubbard model”:

$$\hat{\mathcal{H}} = -t \sum_{\langle lj \rangle \sigma} (c_{j\sigma}^\dagger c_{l\sigma} + c_{l\sigma}^\dagger c_{j\sigma}) + U \sum_I n_{I\uparrow} n_{I\downarrow} + \sum_I (\Delta(-1)^I - \mu)(n_{I\uparrow} + n_{I\downarrow}), \quad (1)$$

where $c_{l\sigma}^\dagger$ ($c_{l\sigma}$) are the usual fermion creation (destruction) operators for spin σ on site l , and $n_{l\sigma} = c_{l\sigma}^\dagger c_{l\sigma}$ is the number operator. t , μ , and U are the electron hopping,

chemical potential, and on-site interaction strength, respectively. The kinetic energy sum is over near neighbor sites $\langle lj \rangle$ on a two-dimensional square lattice. $\Delta(-1)^I$ is a staggered site energy. In the noninteracting limit, $U = 0$, the effect of Δ is to produce a dispersion relation, $E(k) = \pm \sqrt{\epsilon(k)^2 + \Delta^2}$ with $\epsilon(k) = -2t[\cos k_x + \cos k_y]$, which is gapped at half-filling. A considerable amount is known concerning this model in one dimension [6], but the existence of an interaction-driven metallic phase at half-filling is still unresolved even in $d = 1$.

In this Letter we will use DQMC to study the role of interactions in driving a BI-metal transition in the model described by Eq. (1).

Computational methods.—DQMC [9] provides an exact numerical approach to study tight-binding Hamiltonians like the Hubbard model. The partition function Z is first expressed as a path integral by discretizing the inverse temperature β . The on-site interaction is then replaced by a sum over a discrete Hubbard-Stratonovich field [10]. The resulting quadratic form in the fermion operators can be integrated analytically leaving an expression for Z in terms of a sum over all configurations of the Hubbard-Stratonovich field with a summand (Boltzmann weight) which is the product of the determinants of two matrices (one for spin-up and one for spin-down). The sum is sampled stochastically using the Metropolis algorithm. The results capture correlations in the Hubbard Hamiltonian exactly since the systematic “Trotter errors” associated with the discretization of the inverse temperature can easily be extrapolated to zero. Results must also be extrapolated to the thermodynamic limit, as we shall discuss [11].

Equal time operators such as the density and energy are measured by accumulating appropriate elements, and products of elements, of the inverse of the matrix whose determinant gives the Boltzmann weight. We will show results for the spin structure factor,

$$S(\mathbf{k}) = \sum_I e^{i\mathbf{k}\cdot I} \langle (n_{j+\uparrow I} - n_{j+\downarrow I})(n_{j\uparrow} - n_{j\downarrow}) \rangle,$$

which probes magnetic order. For the conductivity, σ_{dc} , we employ an approximate procedure [12] which allows σ_{dc} to be computed from the wave vector \mathbf{q} - and imaginary time τ -dependent current-current correlation function $\Lambda_{xx}(\mathbf{q}, \tau)$ without the necessity of performing an analytic continuation [13],

$$\sigma_{dc} = \frac{\beta^2}{\pi} \Lambda_{xx}(\mathbf{q} = \mathbf{0}, \tau = \beta/2).$$

Here $\beta = 1/T$, $\Lambda_{xx}(\mathbf{q}, \tau) = \langle j_x(\mathbf{q}, \tau) j_x(-\mathbf{q}, 0) \rangle$, and $j_x(\mathbf{q}, \tau)$ the (\mathbf{q}, τ) -dependent current in the x direction, is the Fourier transform of,

$$j_x(\ell, \tau) = i \sum_{\sigma} t_{\ell+\hat{x}, \ell} e^{\tau H} (c_{\ell+\hat{x}, \sigma}^{\dagger} c_{\ell, \sigma} - c_{\ell, \sigma}^{\dagger} c_{\ell+\hat{x}, \sigma}) e^{-\tau H}.$$

This approach has been extensively tested and used for the superconducting-insulator transition in the attractive Hubbard model [12], as well as for metal-insulator transitions in the repulsive model [14].

Results.—We begin by showing the temperature dependence of the conductivity σ_{dc} for increasing values of the interaction strength for $\Delta = 0.5$. In Fig. 1 we see that the insulating behavior at $U = 0$ and $U = 0.2t$, signaled by $d\sigma_{dc}/dT > 0$ at low T , is changed to metallic $d\sigma_{dc}/dT < 0$ at low T when $U = 1$. A further increase of the correlations to $U = 2$ weakens the metallic behavior, which is finally destroyed completely in a transition to a Mott insulator (MI) at $U = 4$. When the band gap is larger ($\Delta = 1$), the screening of the one-body potential is not sufficiently strong for $U = 1$ to cause metallic behavior, as is

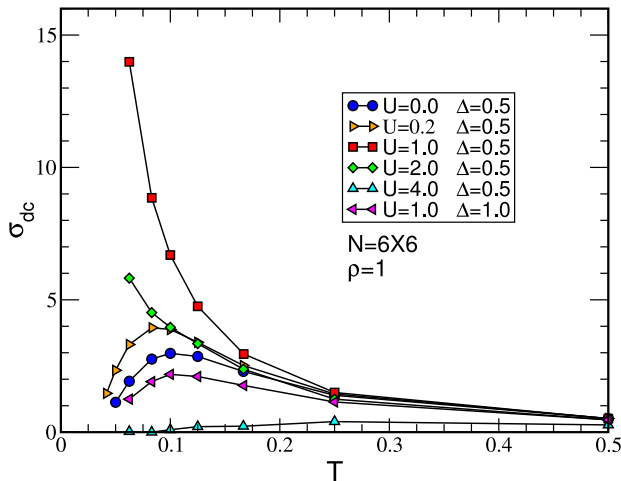


FIG. 1 (color online). The transitions, at half-filling, from a band insulator to metal to MI with increasing U are shown for periodic potential strength $\Delta = 0.5$. At $U = 0$ and $U = 0.2t$ the conductivity σ_{dc} goes to zero as T is lowered. However, for $U = 1t, 2t$ the system is metallic. Mott insulating behavior sets in for $U = 4t$. The lattice size is 6×6 . When $\Delta = 1.0$, the band gap increases and $U = 1t$ is no longer sufficiently large to screen the one-body potential and drive the system metallic.

shown by the corresponding data set in Fig. 1. Unless otherwise mentioned, the lattice size used in the simulations is $N = 6 \times 6$ and the filling is $\rho = 1.0$ (half-filling).

In the single-site ($t = 0$) limit, the ionic Hubbard model is a band insulator for $U < 2\Delta$ and a MI for $U > 2\Delta$. That is, at weak coupling and half-filling, the sites with lower energy $-\Delta$ are doubly occupied and those with higher energy $+\Delta$ are empty, with a gap to further addition of particles set by $2\Delta - U$. At strong coupling, both types of sites are singly occupied, with a “Mott” gap to further addition of particles set by $U - 2\Delta$. At the single special value $U = 2\Delta$ correlations close the gaps [3,8]. Figure 2, which presents results for σ_{dc} for $\Delta = 0.5$, shows that when t is nonzero, this single metallic point is expanded to a finite range of U values. For $U < U_{c1} \approx 0.4t$ the conductivity curves for lower temperature lie below those of higher temperature. The same is true for $U > U_{c2} \approx 2.4t$. In other words, for these interaction strengths, the conductivity is falling as the temperature decreases and, presumably, as T is lowered to zero the conductivity will vanish. Between U_{c1} and U_{c2} the conductivity rises as T is decreased, so that the crossings of the curves signal the transition from BI to metal to MI. Interestingly, however, the largest conductivity remains near $U = 2\Delta = 1$ as one might expect from the $t = 0$ analysis.

The use of DQMC to study the ionic Hubbard model allows us to examine the behavior of intersite correlations, such as the spin-spin correlations and their Fourier transform $S(\mathbf{k})$. Figure 3 shows results for the antiferromagnetic (AF) structure factor $S(\pi, \pi)$ as a function of U for $\beta = 10, 12, 16$. Comparing with Fig. 2 we see that the band insulating and metallic phases are paramagnetic, but that the transition to MI behavior is accompanied by the onset of AF order.

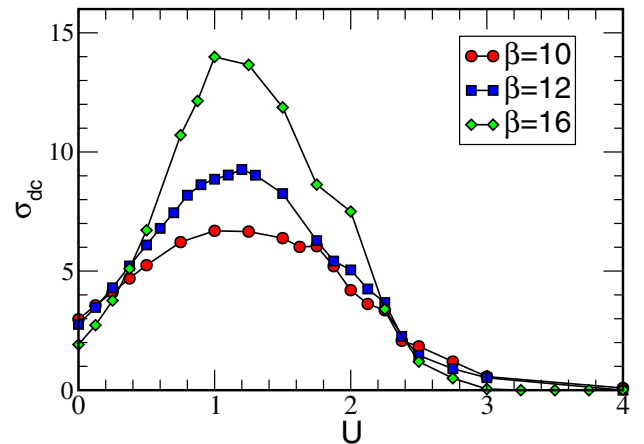


FIG. 2 (color online). The conductivity σ_{dc} at half-filling for $\Delta = 0.5$ is shown as a function of U for three different low temperatures, $\beta = 10, 12, 16$. The band-insulator to metal transition is signaled by the crossing of the curves at $U_{c1} \approx 0.4t$. At $U_{c2} \approx 2.4t$ the three curves cross again, indicating the MI transition.

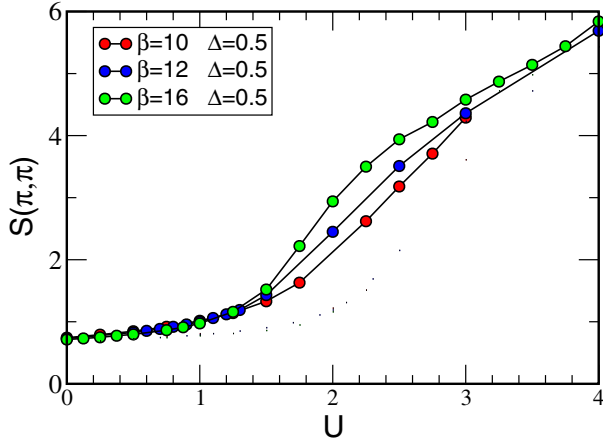


FIG. 3 (color online). The AF structure factor is shown at half-filling as a function of U for $\Delta = 0.5$ and $\beta = 10, 12, 16$.

One way in which the inclusion of such intersite correlations changes the physics in a fundamental way is when the periodic potential is absent, that is, at $\Delta = 0$. Although single-site DMFT can capture AF transitions, when it is restricted to the paramagnetic phase, single-site DMFT concludes the Hubbard model is a metal at weak coupling [15,16]. Indeed, this metallic behavior at $\Delta = 0$ is what is reported in the single-site DMFT treatment of the phase diagram of the ionic Hubbard model [8]. However, it is well known that the $d = 2$ half-filled square lattice Hubbard model, Eq. (1), is an AF insulator at *all* U , even weak coupling. Figure 4 presents our results for the conductivity which confirm this. At all U values shown, σ_{dc}

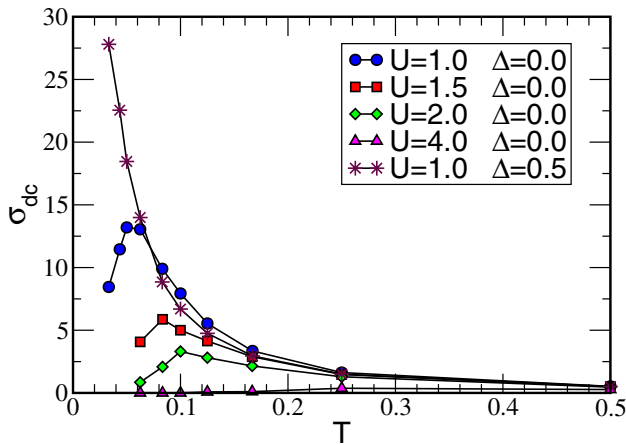


FIG. 4 (color online). The conductivity σ_{dc} is shown as a function of temperature at half-filling. When the periodic potential, and hence the noninteracting band gap, is absent ($\Delta = 0.0$) the square lattice Hubbard model is insulating for *all* U , due to nesting of the Fermi surface. We redisplay data for $\Delta = 0.5$, $U = 1$ from Fig. 1 to emphasize the contrast between the metallic behavior there and the insulating behavior for all U when $\Delta = 0$.

ultimately decreases as T is lowered. Indeed, we have verified that the value of T , where σ_{dc} has its maximum, correlates well with the temperature T_* at which AF correlations begin to rise rapidly. This temperature, like the Néel temperature in the $d = 3$ Hubbard model, is a non-monotonic function of U , falling to small values both at weak and strong coupling. While the insulating nature of the square lattice Hubbard model at weak coupling has been previously shown from QMC studies of the spectral function and spin correlations, this is the first QMC demonstration of the insulator based on a calculation of σ_{dc} .

It is interesting to note that while all the $\Delta = 0$ curves have a positive low temperature slope, $d\sigma_{dc}/dT > 0$, a distinction between the origins of insulating behavior in the weak and strong coupling regions is clearly evident. At small U , where the “Slater” gap originates due to AF correlations, σ_{dc} attains a large value before turning over as T is lowered. When U is bigger, so that a “Mott” gap separating upper and lower Hubbard bands begins to emerge, σ_{dc} is much reduced.

While DQMC allows us to look at intersite correlations and concomitant phenomena like antiferromagnetism, the method employs lattices of finite size, unlike DMFT which directly probes the thermodynamic limit. Thus, it is important to verify that the metallic phase we observe persists on larger lattices. In Fig. 5 we show results for σ_{dc} as a function of temperature in the metallic phase for lattices up to 12×12 . The rise in σ_{dc} with decreasing T is seen to occur for all the lattices studied. We comment that it is not surprising that we find the lattice size has a rather substantial influence on the conductivity for these parameters, since it is known that such finite size effects are larger at weak coupling.

Conclusions.—We have presented determinant quantum Monte Carlo studies of the two-dimensional ionic Hubbard

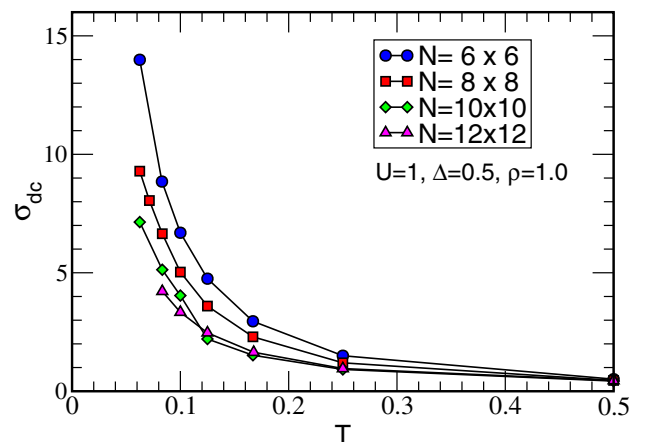


FIG. 5 (color online). The conductivity at half-filling is shown for different lattice sizes for $U = 1$, close to the point where the system is most metallic for periodic potential $\Delta = 0.5$. (See Fig. 2). Although σ_{dc} decreases with increasing lattice sizes, the signature of metallic behavior ($d\sigma_{dc}/dT < 0$) is unchanged.

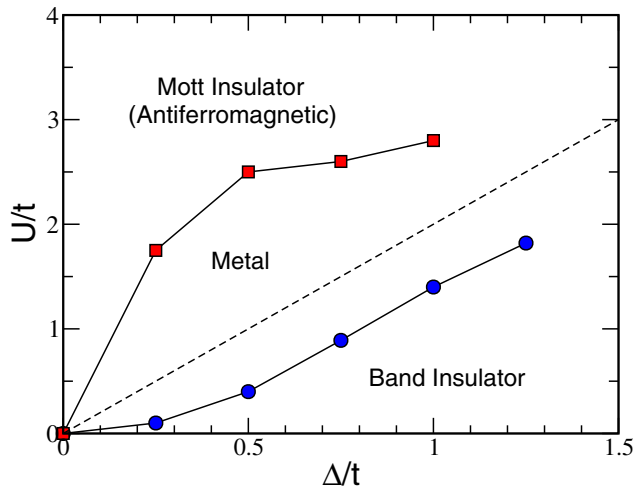


FIG. 6 (color online). The phase diagram of the ionic Hubbard model. Symbols are the result of our QMC simulations. The dashed line is the strong coupling ($t = 0$) phase boundary between band-insulator and Mott insulator.

Hamiltonian which demonstrate that interactions can drive a band-insulator metallic. This work complements DMFT studies by including intersite AF correlations which qualitatively alter the ground state phase diagram.

We have focused most of our results on $\Delta = 0.5$. However, we have also performed simulations sweeping U at $\Delta = 0.25$ and $\Delta = 1.00$. The emerging phase diagram is shown in Fig. 6. There are several key differences with that obtained with single-site DMFT [8]. First, as we have emphasized, the behavior along the $\Delta = 0$ axis is significantly altered. Contrary to DMFT, the inclusion of intersite magnetic fluctuations yields an AF insulating phase for all U . This difference, while important, is however expected since single-site DMFT is unable to capture order which requires multiple sites. Indeed, a recent preprint [17] reports results for the ionic Hubbard model using cluster DMFT to incorporate intersite correlations. When DMFT is extended in this way, the resulting phase diagram matches ours qualitatively and quantitatively very well: these authors also find a Mott phase along the entire $\Delta = 0$ axis of the phase diagram. Our results and cluster DMFT both find the intermediate phase is centered roughly around the strong coupling boundary line $U = 2\Delta$ (dashed line in Fig. 6), and have similar extent.

There is still an important open issue concerning the precise nature of the intermediate phase. Our results suggest, in agreement with single-site DMFT [8], that this phase is metallic, while Kancharla *et al.* suggest a bond ordered phase. Nevertheless, all three approaches agree on

the vanishing of the gap in the phase located between the band and Mott insulators.

We acknowledge support from NSF DMR 0312261, and useful input from S. A. Clock.

-
- [1] P. A. Lee and T. V. Ramakrishnan, *Rev. Mod. Phys.* **57**, 287 (1985); D. Belitz and T. R. Kirkpatrick, *Rev. Mod. Phys.* **66**, 261 (1994); “Metallic Behavior and Related Phenomena in Two Dimensions,” E. Abrahams, S. V. Kravchenko, and M. P. Sarachik, *Rev. Mod. Phys.* **73**, 251 (2001); S. V. Kravchenko and M. P. Sarachik, *Rep. Prog. Phys.* **67**, 1 (2004).
 - [2] This problem is also under current investigation for bosonic systems. See, for example, D. Jaksch, C. Bruder, J. I. Cirac, C. W. Gardiner, and P. Zoller, *Phys. Rev. Lett.* **81**, 3108 (1998); P. Buonsante and A. Vezzani, *Phys. Rev. A* **70**, 033608 (2004).
 - [3] V. G. Rousseau *et al.*, *Phys. Rev. B* **73**, 174516 (2006).
 - [4] T. Egami, S. Ishihara, and M. Tachiki, *Science* **261**, 1307 (1993).
 - [5] N. Nagaosa and J. Takimoto, *J. Phys. Soc. Jpn.* **55**, 2735 (1986); **55**, 2745 (1986); N. Nagaosa, *ibid.* **55**, 2754 (1986), and references therein.
 - [6] J. Hubbard and J. B. Torrance, *Phys. Rev. Lett.* **47**, 1750 (1981); G. Ortiz and R. M. Martin, *Phys. Rev. B* **49**, 14202 (1994); R. Resta and S. Sorella, *Phys. Rev. Lett.* **74**, 4738 (1995); *Phys. Rev. Lett.* **82**, 370 (1999); M. Fabrizio, A. O. Gogolin, and A. A. Nersisyan, *Phys. Rev. Lett.* **83**, 2014 (1999); T. Wilkens and R. M. Martin, *Phys. Rev. B* **63**, 235108 (2001); C. D. Batista and A. A. Aligia, *Phys. Rev. Lett.* **92**, 246405 (2004).
 - [7] S. Ishihara, T. Egami, and M. Tachiki, *Phys. Rev. B* **49**, 8944 (1994).
 - [8] A. Garg, H. R. Krishnamurthy, and M. Randeria, *Phys. Rev. Lett.* **97**, 046403 (2006).
 - [9] R. Blankenbecler, D. J. Scalapino, and R. L. Sugar, *Phys. Rev. D* **24**, 2278 (1981).
 - [10] J. E. Hirsch, *Phys. Rev. B* **31**, 4403 (1985).
 - [11] The advantages of DMFT relative to DQMC are that DMFT works in the thermodynamic limit and that the “sign problem” is considerably less severe.
 - [12] N. Trivedi, R. T. Scalettar, and M. Randeria, *Phys. Rev. B* **54**, R3756 (1996).
 - [13] D. J. Scalapino, S. R. White, and S. Zhang, *Phys. Rev. B* **47**, 7995 (1993).
 - [14] P. J. H. Denteneer, R. T. Scalettar, and N. Trivedi, *Phys. Rev. Lett.* **83**, 4610 (1999); *Phys. Rev. Lett.* **87**, 146401 (2001).
 - [15] A. Georges *et al.*, *Rev. Mod. Phys.* **68**, 13 (1996).
 - [16] T. Pruschke, M. Jarrell, and J. K. Freericks, *Adv. Phys.* **44**, 187 (1995).
 - [17] S. S. Kancharla and E. Dagotto, *Phys. Rev. Lett.* **98**, 016402 (2007)..